

## Time-Resolved Fluorescence Studies of Dityrosine in the Outer Layer of Intact Yeast Ascospores

A. J. Kungl,\* A. J. W. G. Visser,† H. F. Kauffmann,\* and M. Breitenbach§

\*Institut für Physikalische Chemie der Universität Wien, Währingerstraße 42, A-1090 Wien, Austria; †Department of Biochemistry, Agricultural University, Dreijenlaan 3, NL-6703 HA Wageningen, The Netherlands; and §Abteilung für Genetik und Entwicklungsbiologie, Universität Salzburg, Hellbrunnerstraße 34, A-5020 Salzburg, Austria

**ABSTRACT** The (time-resolved) fluorescence properties of dityrosine in the outermost layer of the spore wall of *Saccharomyces cerevisiae* were investigated. Steady-state spectra revealed an emission maximum at 404 nm and a corresponding excitation maximum at 326 nm. The relative fluorescence quantum yield decreased with increasing proton concentration. The fluorescence decay of yeast spores was found to be nonexponential and differed pronouncedly from that of unbound dityrosine in water. Analysis of the spore decay recorded at  $\lambda_{\text{ex}} = 323$  nm and  $\lambda_{\text{em}} = 404$  nm by an exponential series (ESM) algorithm revealed a bimodal lifetime distribution with maxima centered at  $\tau_1^c = 0.5$  ns and  $\tau_2^c = 2.6$  ns. The relative amplitudes of the two distributions are shown to depend on the emission wavelength, indicating contributions from spectrally different dityrosine chromophores. On quenching the spore fluorescence with acrylamide, a downward curvature of the Stern-Volmer plot was obtained. A multitude of chromophores more or less shielded from solvent in the spore wall is proposed to account for the nonlinear quenching of the total spore fluorescence. Analysis of the fluorescence anisotropy decay revealed two rotational correlation times ( $\varphi_1 = 0.9$  ns and  $\varphi_2 = 30.6$  ns) or a bimodal distribution of rotational correlation times (centers at 0.7 ns and 40 ns) when the data were analyzed by the maximum entropy method (MEM). We present a model that accounts for the differences between unbound (aqueous) and bound (incorporated in the spore wall) dityrosine fluorescence. The main feature of the photophysical model for yeast spores is the presence of at least two species of dityrosine chromophores differing in their chemical environments. A hypothetical photobiological role of these fluorophores in the spore wall is discussed: the protection of the spore genome from mutagenic UV light.

### INTRODUCTION

Dityrosine has been found in a wide variety of hard and/or protective biological structures, among them the hard fertilization membrane of the sea urchin egg (Foerder and Shapiro, 1977) and the outermost layer of the spore wall of yeast (Briza et al., 1986). Dityrosine seems to arise by an oxidative cross-linking reaction between two L-tyrosine residues (see Fig. 1), either in proteins that are preassembled in the layer to be “hardened” or between tyrosine residues that are part of a nonprotein precursor, to the final insoluble structural biopolymer (as for yeast, P. Briza and M. Breitenbach, unpublished results). In yeast, after cross-linking, another interesting reaction takes place: epimerization resulting in D,L-dityrosine, which makes up nearly half of the final product. The chemical properties of dityrosine are certainly aiding its resistance function in biopolymers: the *o,o'*-biphenol structure is relatively rigid, and even rotation along the biphenolic bond is strongly hindered at ambient temperatures (Kungl et al., in press), the peptide bonds of dityrosine are resistant against most proteases, and the D-configuration of D,L-dityrosine further increases protease resistance. The phenolic -OH groups of dityrosine

are much more acidic than that of tyrosine, which could lead to strong electrostatic binding to positively charged structural polymers. The  $\pi$  electron system of dityrosine displays an absorption maximum at 320 nm in alkaline aqueous solutions, which is nearly coincident with the most important mutagenic wavelength in sunlight at sea level, resulting in strong natural fluorescence at 405 nm.

Time-resolved fluorescence measurements have become a valuable tool in modern biochemistry (Beechem and Brand, 1985). Regarding proteins, the intrinsic fluorescence of tryptophan and tyrosine (Creed, 1984a, b) has revealed aspects of chromophore environment and the dynamics of the macromolecule on fluorescence time scales (Eftink, 1991a). Special emphasis has been given to the interpretation of the nonexponential fluorescence decay of proteins (Royer, 1993). Commonly, deviations from a monoexponential decay are attributed to a multitude of deactivation channels referring to a multitude of microenvironments (Hutnik and Szabo, 1989). This dispersion might arise from chromophores of the same species residing in different sites of the protein. However, a protein containing a single chromophore can yield a nonexponential fluorescence decay too, if dynamical changes in the protein matrix affect the chromophore during its fluorescence lifetime. Moreover, picosecond and sub-picosecond energy- and electron-transport processes might constitute to the complexity of the transients (Harris and Hudson, 1990). This has been the subject of intense research by time-resolved fluorescence spectroscopy during the last years (Eftink, 1991a).

Received for publication 1 March 1994 and in final form 29 April 1994.

Address reprint requests to A. J. Kungl, Sandoz Research Institute, Dept. Antiretroviral Therapy (ART), Brunnerstraße 59, A-1235 Wien, Austria. Tel.: 43-1-867511-259; Fax: 43-1-867511-727; E-mail: kungl\_a@a1.wienr1.sandoz.com.

© 1994 by the Biophysical Society

0006-3495/94/07/309/09 \$2.00

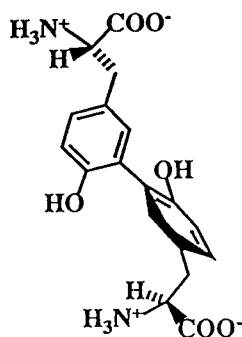


FIGURE 1 Structure of LL-dityrosine.

Recently, it has been pointed out that complex, nonexponential fluorescence relaxation patterns result from a distribution of deactivation channels. Thus, the common multiexponential reconvolution procedure should in such cases be regarded as a pure curve parametrization (James and Ware, 1985, 1986). For the analysis of protein fluorescence, Alcalá et al. (1987a–c) have implemented trial probability functions for conformational transition frequencies in frequency domain data analysis, and the distribution parameters have been evaluated by means of an iterative nonlinear least-squares algorithm. Additionally, fluorescence lifetime distribution patterns from protein fluorescence have been reconstructed by means of entropy maximization (Skilling and Gull, 1985) adapted to fluorescence decay analysis by Livesey and Brochon (Livesey and Brochon, 1987; Vincent et al., 1988; Merola et al., 1989).

Previously, we have investigated the fluorescence characteristics of dityrosine (Kungl et al., 1992), which is the predominant chromophore in the outermost layer of yeast spores (Briza et al., 1986). The fluorescence decay of aqueous dityrosine was found to be highly nonexponential and could be best described by three exponential terms or by a trimodal lifetime distribution, respectively. The pronounced sub-nanosecond rise-term in the transients recorded at  $\lambda_{em} \geq 390$  nm was shown to be the result of a consecutive reaction in the excited state of the molecule. We suggested that the excited biphenolic monoanion of dityrosine has a high tendency of incorporating the lone-pair electrons of the phenolate oxygen into the aromatic system, thus losing aromaticity caused by a quinoid structure. Moreover, this structure is coplanar. The monoanion, which is a necessary prerequisite for the excited state reaction to occur, is generated either in the ground state at pH > 7, or in an excited state deprotonation on a picosecond timescale at lower pH values.

In this paper, we will show that, although the stationary spectra of an alkaline aqueous suspension of yeast spores are similar to those of dityrosine, the time-resolved fluorescence spectra differ pronouncedly. A model is introduced that proposes at least *two* different environments for the chromophore. Two rotational correlation times obtained by fluorescence anisotropy measurements of intact yeast spores also confirm two dynamical ranges for the fluorophore caused by different environments. Distributional analysis has been ap-

plied to the fluorescence decay as well as to the anisotropy decay of the yeast spores.

## MATERIALS AND METHODS

For spore purification, strain AP3, a heterothallic diploid was presporulated and sporulated on 1% potassium acetate as described previously (Hartig et al., 1981). Mature asci and remaining nonsporulated cells were treated with glucosylase (Sigma, Deisenhofen, Germany) to lyse vegetative cell walls and ascus walls. The spores which were resistant to glucosylase were further purified by centrifugation through a density step-gradient of Percoll (Amersham, Buckinghamshire, England) as described previously (Esposito et al., 1991). The spores contained less than 1% remaining small vegetative cells as determined by counting in a hemocytometer under a microscope. The spores were washed free of gradient material and kept in an aqueous solution of 0.1% Triton X100 to prevent clumping. Spore viability was still near 100% after keeping the spores at 4°C for 1 year. Before fluorescence measurements, Triton X100 was removed by several steps of washing with H<sub>2</sub>O and centrifugation.

Steady-state fluorescence and fluorescence excitation spectra were collected on a Hitachi Perkin-Elmer MPF 4 spectrometer (Hitachi, Tokyo, Japan). The excitation wavelength of dityrosine fluorescence ranged from 260 to 350 nm depending on the pH of the solution. In general, slits giving bandwidths of 2–4 nm were used. Fluorescence excitation spectra of dityrosine were monitored at wavelengths  $\lambda_{em} = 320$ –540 nm. Spectra presented in this study are uncorrected.

Time-resolved fluorescence measurements in the nanosecond time range were performed on a serial PRA 3000 transient configuration (Photochemical Research Association, London, Ontario, Canada). The full width at half-maximum of the thyatron-gated hydrogen flash-lamp instrumental function was typically 1.3 ns. Fluorescence photons were detected by a Hamamatsu R928 photomultiplier (Hamamatsu, Hamamatsu City, Japan) and time-correlated by single-photon counting (O'Connor and Phillips, 1984). The time-to-amplitude converted output signals were collected in a Tracor Northern TN 1750 (Tracor Northern, Middleton, NJ) multichannel analyzer. The fluorescence histogram was then transferred to a MicroVAX II (Digital Equipment Corporation, Maynard, MA) for data analysis.  $2 \times 10^4$  counts were usually collected in the peak channel maximum. No significant nonlinearities in the TAC could be detected. Instrumental response functions were collected at the excitation as well as at the emission wavelength to rule out an energy-dependent delay (photomultiplier color effect).

## Data analysis

A modified exponential series method (Landl et al., 1991) was used to evaluate a potential distribution of fluorescence lifetimes from a (nonexponential)  $\delta$ -pulse fluorescence response  $F(t)$ . In the ESM,  $F(t)$  is approximated by a series of exponentials with fixed lifetimes  $\tau_n$  spaced equally or logarithmically over the time scale of fluorescence

$$F(t) = \sum_n a_n e^{-t/\tau_n}. \quad (1)$$

From the convolution integral

$$H(t) = L(t) \otimes F(t), \quad (2)$$

the corresponding discrete set of amplitudes  $a_n$  (distribution) is then evaluated in a linear, least-squares optimization,  $H(t)$  and  $L(t)$  being the raw data and the lamp-instrumental response function, respectively. 70 terms were usually set in the following analysis. A rectangular distribution of initial values was applied in the ESM to avoid preconceived bias into the computation.

The method was shown to work well on high-accuracy synthetic and experimental data. No cutoff is required for deleting amplitudes of values close to zero during reconvolution. Contrary to other exponential series techniques, our method is not restricted to positive amplitudes. Also, rise terms can be investigated with the drawback of slight oscillations, which are numerical artifacts. Details of the method are given elsewhere (Landl et al., 1991).

Time-resolved fluorescence anisotropy experiments on the picosecond time scale were obtained as described earlier (van Hoek et al., 1987). An argon ion laser (Coherent Radiation CR18) was mode-locked, and a DCM dye laser (modified CR590) was synchronously pumped and frequency-doubled to have 340-nm radiation. To decrease the 76-MHz repetition rate of exciting light pulses to 596 kHz, an electro-optic modulator set-up was used (van Hoek and Visser, 1981). The energy of exciting light pulses was in the subnanjoule region. A Baird Atomic 402.3 nm interference filter was combined with a KV389 cutoff filter (Schott) to select fluorescence emission, and a fast 90° rotating sheet polarizer (Polaroid) was used to select emission polarized vertically or horizontally with respect to the polarization direction of the excitation light. Fluorescence photons were detected using a Hamamatsu R1645U-01 microchannel plate detector and further processed by time-correlated single photon counting. In two subgroups (1024 channels each) of the memory of a multichannel analyzer (Nuclear Data ND66) data were collected of semi-simultaneously recorded data of vertically and horizontally polarized fluorescence. A reference compound with a few picoseconds fluorescence lifetime was measured before and after the fluorescence experiment, and the average of the two was taken in the deconvolution procedure. In our case, the reference compound was a pseudoazulene with a lifetime of 10 ps (Visser et al., 1988). Data analysis was performed as detailed by Vos et al. (1987) and with the software from Maximum Entropy Data Consultants Inc. (Cambridge, England).

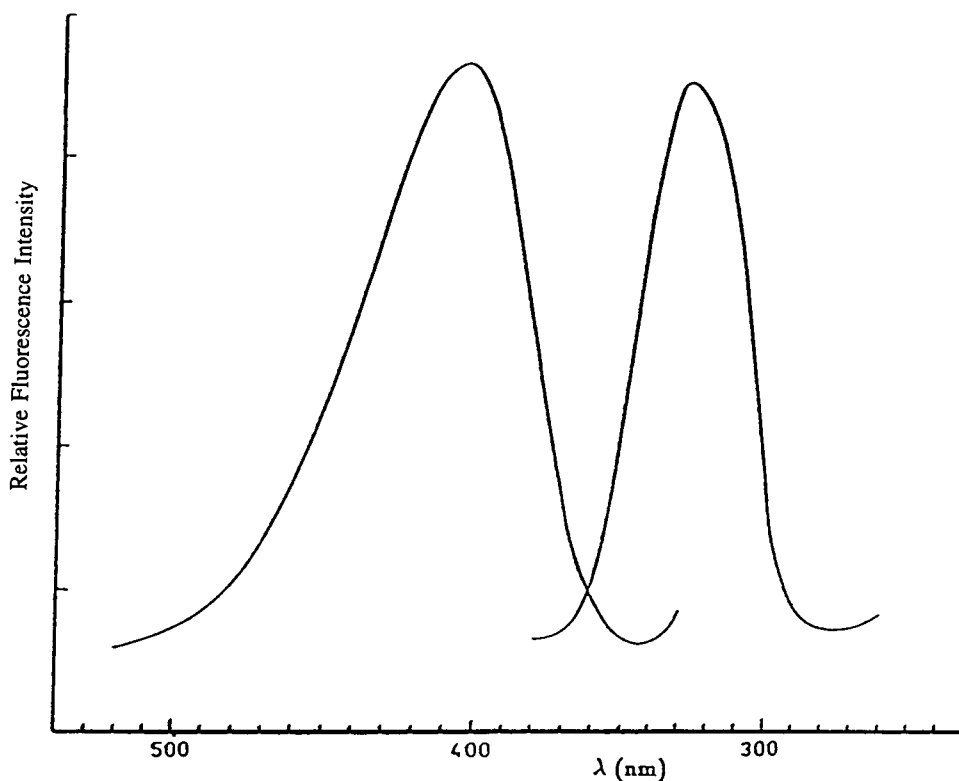
## RESULTS

The quantum yield of an aqueous suspension of yeast spores increased with decreasing proton concentration, yielding high values above pH 8 and low values below pH 7. The fluorescence emission maximum was found at 404 nm, the corresponding excitation band being located at 326 nm (Fig. 2). Compared with aqueous dityrosine this means small band shifts ( $\lambda_{\text{ex}}^{\text{max}} = 320$  nm and  $\lambda_{\text{em}}^{\text{max}} = 405$  nm found for aqueous dityrosine) as well as broadening of the fluorescence bands in the spore wall.

Through all (time-resolved) fluorescence experiments, the spore suspensions were stirred to keep the overall distribution of spores in water constant. In Fig. 3 A, time-resolved fluorescence data of an alkaline spore suspension are shown which were recorded at  $\lambda_{\text{ex}} = 326$  nm and  $\lambda_{\text{em}} = 404$  nm. Because of the low quantum yield of the spores as compared with unbound dityrosine, we were not able to collect more than  $2 \times 10^4$  counts in the peak maximum channel. The decay of yeast spores was found to be nonexponential. To fit the recorded decays properly, two or three exponential terms were needed, the necessary number of exponentials being dependent neither on the excitation/emission wavelength nor on the pH of the suspension. Because of this, without any trend, varying number of exponentials necessary for a good fit, we can conclude that discrete exponentials represent a curve parametrization that is better described by a distribution of lifetimes. Indeed, the complex polypeptide matrix should give rise to a distribution of conformational transition frequencies, making an analysis of the fluorescence decay by an exponential series method more reliable (James and Ware, 1986; Alcalá et al., 1987a–c).

In Fig. 3 B, the ESM spectrum of the spore transient recorded at pH 8–9 (compare Fig. 3 A) is shown. It was not necessary to allow for negative amplitudes in the analysis of the time-resolved fluorescence data. A regularization parameter of 1 (Landl et al., 1991) was always applied to keep artificial oscillations low. Two well separated lifetime distributions were found, located at  $\tau_1^c = 0.5$  ns and at  $\tau_2^c = 2.6$  ns when the fluorescence was collected at the maximum intensity at 404 nm on excitation at 326 nm (Fig. 3). Fixing the excitation wavelength at this value and

FIGURE 2 Steady-state fluorescence spectra of yeast spores in an alkaline (pH 8–9) suspension: fluorescence emission recorded at  $\lambda_{\text{ex}} = 326$  nm, and fluorescence excitation recorded at  $\lambda_{\text{em}} = 404$  nm. The uncorrected spectra are presented.



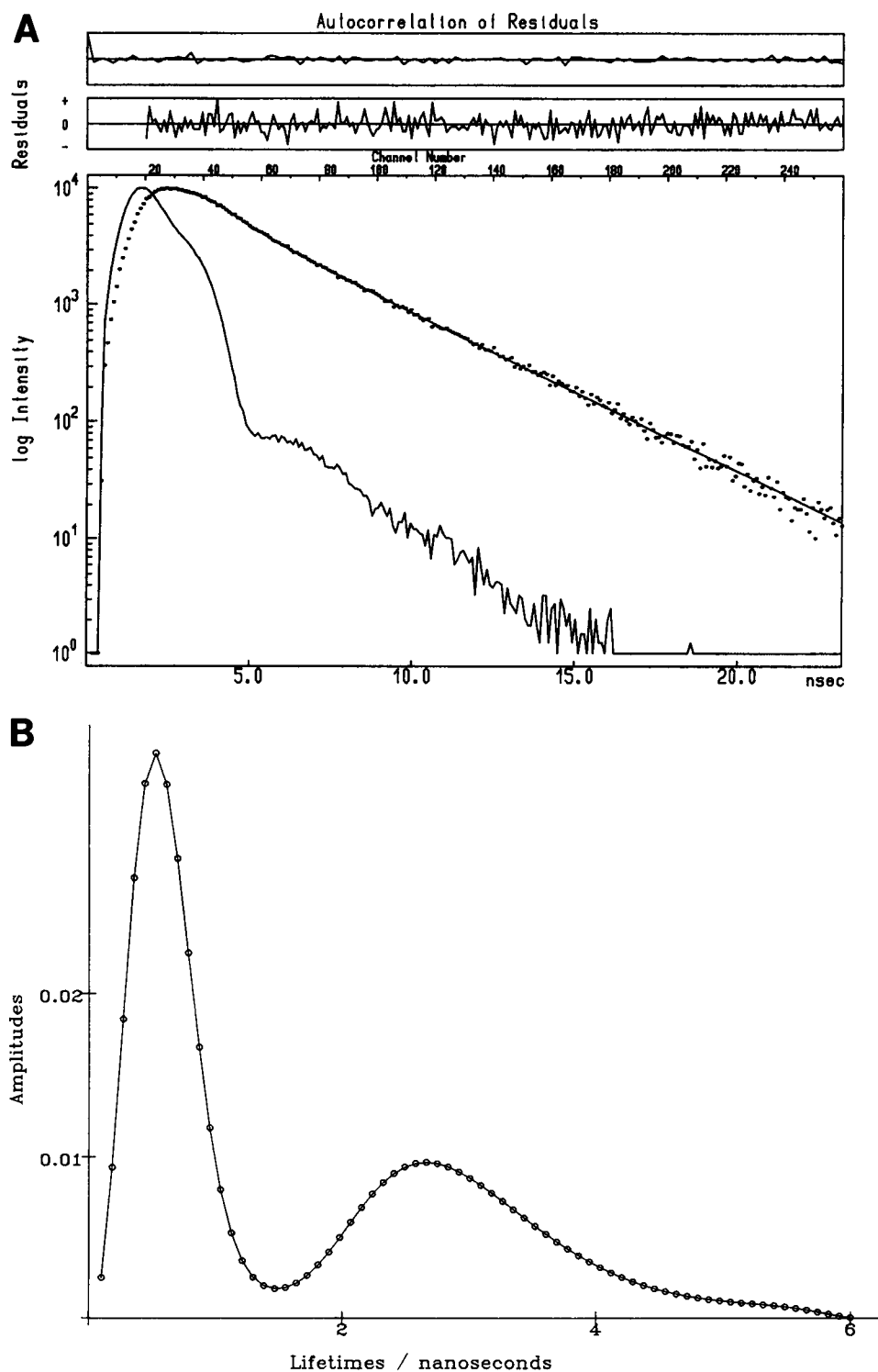


FIGURE 3 (A) Transient of an alkaline yeast spore suspension (pH 8–9) recorded at  $\lambda_{ex} = 326$  nm and  $\lambda_{em} = 404$  nm. The dots represent the raw data, the solid line is the instrumental response (scatter), and the bold line is the best fit obtained by ESM analysis ( $\chi^2 = 1.1$ ). (B) corresponding ESM analysis with 70 lifetimes linearly spaced over a time range of 0.1–6 ns.

varying the emission wavelength results in a change of the relative distributional amplitude ratio with the lifetime centers nearly unchanged. The reliability of our PRA time-resolved fluorescence set-up for recovering lifetime distributions even in the sub-nanosecond time domain, the resolution being dependent upon the data quality, has been previously demonstrated by comparative experiments on a laser single photon counting set-up (Kungl et al., 1992). The

small shift observed for the central lifetime values can be accounted for by the increasing overlap of the distributions at  $\tau_1^c$  and  $\tau_2^c$ .

To see whether we can resolve individual time-resolved signals from spectrally different chromophores, we measured the sample at the blue and at the red edge of the corresponding stationary excitation and emission spectrum (compare Fig. 2). ESM analysis of the fluorescence data

collected at 333 nm with the excitation set at 285 nm revealed again two lifetime distributions. But the long-lived contribution to the overall decay was very small (see Fig. 4 A). A single but broad lifetime distribution was obtained with a central value at 2.1 ns when the sample was excited at 350 nm and the fluorescence was collected at 430 nm (see Fig. 4 B).

The fluorescence quenching of a yeast spore suspension by acrylamide yielded a nonlinear Stern-Volmer plot when  $(F_0/F)$  was plotted against  $c_{\text{acr}}$  (Fig. 5), according to the Stern-Volmer equation  $(F_0/F) = 1 + k_q \cdot \tau_0 \cdot c_{\text{acr}}$ , where  $F_0$  is the fluorescence in the absence of quencher,  $c_{\text{acr}}$  is the concentration of acrylamide, and  $(k_q \cdot \tau_0) = K_D$  is the Stern-Volmer constant. Instead of the linear plot observed for the

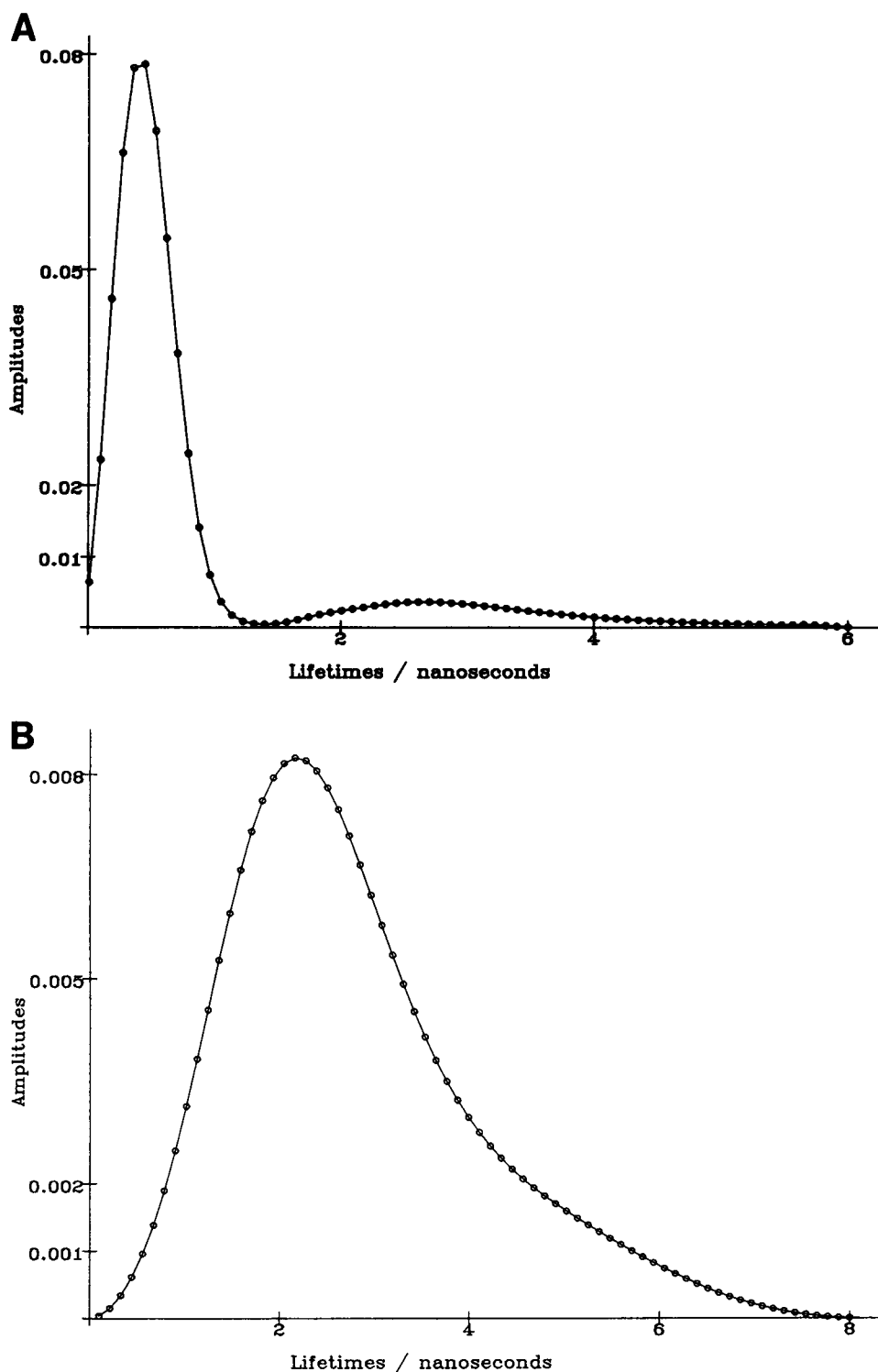
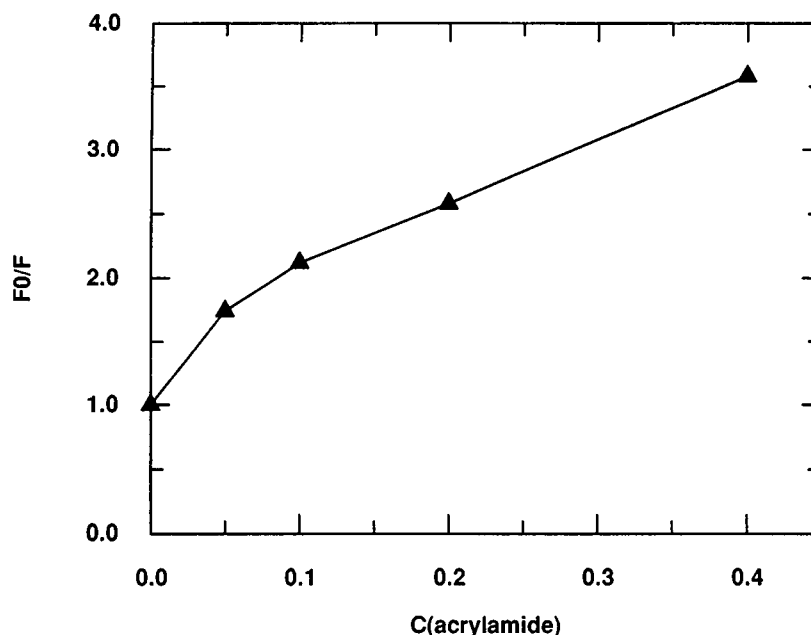


FIGURE 4 ESM analysis of nano-second time-resolved fluorescence data of an alkaline spore suspension (pH 8–9) recorded (A) at  $\lambda_{\text{ex}} = 285$  nm and  $\lambda_{\text{em}} = 333$  nm ( $\chi^2 = 1.2$ ) and (B) at  $\lambda_{\text{ex}} = 350$  nm and  $\lambda_{\text{em}} = 430$  nm ( $\chi^2 = 1.1$ ).

FIGURE 5 Stern-Volmer Plot of spore-fluorescence quenched with acrylamide (for further details, see text).



dityrosine fluorescence in water (A. J. Kungl, unpublished results), a downward curvature was observed (Fig. 5). Trials to adjust the data to several other quenching equations (Eftink, 1991b) failed in every case. No linear plot for quenching the dityrosine fluorescence in yeast spores by acrylamide was found.

On analyzing the acrylamide-quenched time-resolved fluorescence data by ESM, two effects were observed when the concentration of acrylamide was increased from 0 to 0.4 M: (a) the relative amplitudes (see Fig. 3 B) of the lifetime distributions changed towards a more than 10-fold decrease of the long-lived distribution, and (b) the central value of the long-lived distribution  $\tau_2^c$  shifted from 2.8 to 1.8 ns, whereas  $\tau_1^c$  remained unchanged at 0.48 ns. This can be attributed to *two* differently located chromophore classes being represented by *two* lifetime distributions, one accessible to a freely diffusing quencher like acrylamide and the other one hidden. The bimolecular rate constant for quenching of the solvent-accessible dityrosine-chromophores was estimated on the basis of the ESM analysis to be  $1.19 \times 10^9 \text{ M}^{-1} \text{ s}^{-1}$ .

Analysis of the time-resolved fluorescence anisotropy spectra of an alkaline spore suspension yielded two rotational correlation times (the corresponding relative amplitudes are given in brackets):  $\varphi_1 = 0.90 \text{ ns}$  (0.02) and  $\varphi_2 = 30.6 \text{ ns}$  (0.06). Assuming again that two dityrosine chromophore classes are responsible for these two exponential terms, 75% have a slower motion according to the amplitude.  $r_0$  has been extrapolated to an initial value of 0.288. In Fig. 6, the distributional analysis of the time-resolved anisotropy decay by the maximum entropy method (Livesey and Brochon, 1987) is shown. 100 rotational correlation times were spaced logarithmically over a time scale ranging from 0.05 to 100 ns. A broad distribution of rotational correlation times centered at 40 ns represents the main contribution (70%) to the anisotropy

decay, whereas a sharp distribution at 0.7 ns is the minor contribution (30%). Any influence on the analysis of the fluorescence decay caused by scattering of the spores has been ruled out by setting the excitation wavelength at 340 nm and collecting the emission at 402 nm.

## DISCUSSION

We have previously shown that LL-dityrosine undergoes an excited state reaction in aqueous media (Kungl et al., 1992). This reaction has been characterized by steady-state and time-resolved fluorescence measurements. A Stokes' shift of 85 nm (in alkaline solution) was indicative for a consecutive (irreversible) reaction in the excited state leading from a twisted, monoanionic (generated by ground or excited state deprotonation of a phenolic hydroxyl group) precursor to a coplanar, electronically conjugated successor. The latter showing an emission maximum at 405 nm and a fluorescence lifetime of 4.6 ns. The precursor could not be resolved in the steady-state spectra, but a lifetime of 1.6 ns could be assigned by time-resolved emission spectroscopy. The build-up of successor has been followed by time-resolved measurements, too. A sub-nanosecond rise time has been found when transient data of dityrosine recorded at 405 nm were analyzed. The rise time is the reciprocal value of the rate constant for the excited state reaction.

A similar Stokes' shift has been found for dityrosine in intact yeast spores at alkaline pH values. The value of 78 nm is significantly smaller than the 85 nm found for dityrosine in water. We know that the fluorescence response of the chromophore is very sensitive to its chemical environment (A. J. Kungl, unpublished data). When *o,o*-biresole, a dityrosine-homolog, is dissolved in solvents with decreasing polarity, the emission maximum shifts to lower wavelengths

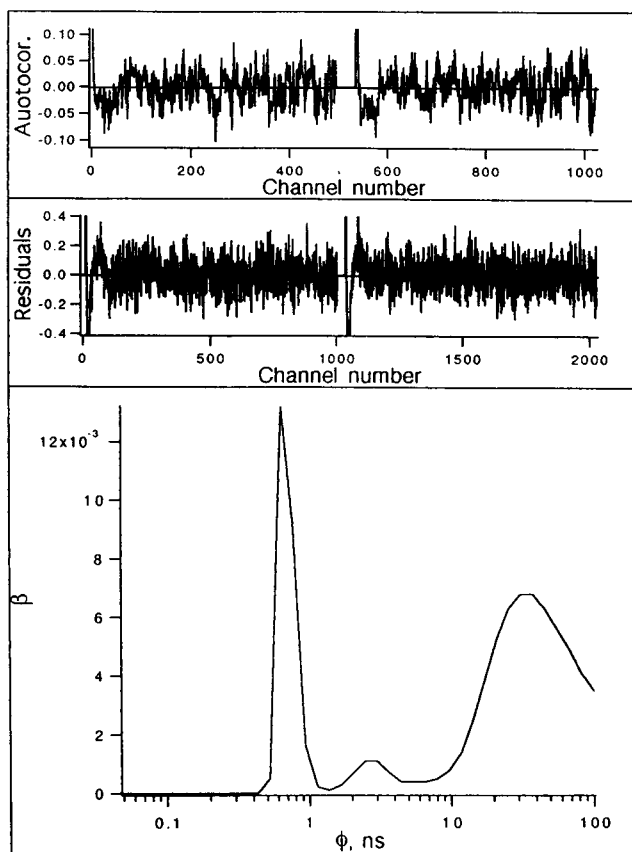


FIGURE 6 Analysis of the time-resolved anisotropy decay of yeast spores by the MEM method. 100 rotational correlation times were spaced logarithmically over a time scale ranging from 0.05 to 100 ns ( $\chi^2 = 1.96$ ).

compared with an aqueous solution. The rather large shift of bicresole fluorescence from 404 nm in water to 350 nm in cyclohexane is accompanied by a slight shift in the respective excitation bands from 320 to 310 nm. A fluorescence-band shift is thus a good indicator for the solvation (chemical environment) of dityrosine-like chromophores.

The relative fluorescence quantum yield of yeast spores was shown to increase with increasing pH, whereas nearly no emission could be detected in acidic solutions. The pH in sporulating yeast cultures is approximately 8 compared with growing yeast cultures with a pH  $\sim 6$ . Thus, physiological conditions, which were chosen throughout all measurements, are accompanied by strong fluorescence emission.

Regarding the fluorescence decay of yeast spores, we would have expected a rise term similar to the one found in the decay of aqueous dityrosine because of the similar Stokes' shift detected in both systems. From independent measurements, we know that the rate of the excited state reaction depends on the state of solvation (A. J. Kungl, unpublished data). Two factors govern the excited state reaction: (1) the capacity of the solvent to accept protons from the chromophore due to ground or excited state deprotonation (dependent on pH), and (2) the rate of solvent relaxation after excitation (Demchenko, 1992). If the excited state re-

action of dityrosine is still about to occur in yeast spores, this means that in the spore wall is (1) a suitable proton acceptor (fluorescence band at 404 nm) and (2) there is a chemical environment that governs a much faster rate of the excited state reaction compared with dityrosine in solution. We assume that the photophysical reaction of dityrosine within the spore wall happens within a few picoseconds or even faster, below the resolution of our instrumentation. Therefore, the excited state reaction proposed for dityrosine in water which leads to an energetically low emissive successor state should still be valid for dityrosine incorporated in the macromolecular matrix of yeast spores. This explains the similar steady-state spectra of the bound and unbound fluorophore.

When the fluorescence decay of an alkaline yeast spore suspension was recorded at the maximum of absorption (326 nm) and at the maximum of fluorescence intensity (404 nm), two well separated lifetime distributions were found centered at  $\tau_1^c = 0.5$  ns and  $\tau_2^c = 2.6$  ns (Fig. 3 B). This ESM pattern is different from the ESM distributional analysis of dityrosine in water (Kungl et al., 1992). There, three lifetime distributions centered at 0.3, 1.5, and 4.5 ns were found, the first of which was associated to negative preexponential terms. The latter two distributions are the lifetimes of the precursor and successor of the excited state reaction. From the ESM analysis of the spore fluorescence, we conclude that we are not able to resolve the details of the complex photophysics of dityrosine when it is bound to the macromolecular matrix of the spore wall.

We rather interpret the nonexponential fluorescence response of yeast spores as resulting from overlapping signals of at least two dityrosine chromophores which differ by their location and, thus, by their spectral behavior (Royer et al., 1990). We found the amplitudes of the lifetime distributions centered at  $\tau_1^c$  and  $\tau_2^c$  dependent on the excitation/emission wavelength (Fig. 4). With  $\lambda_{ex} = 285$  nm and  $\lambda_{em} = 333$  nm, two lifetime distributions were found, the long-lived contribution being very small (Fig. 4 A). With  $\lambda_{ex} = 350$  nm and  $\lambda_{em} = 430$  nm, only a single but broad lifetime distribution was found (Fig. 4 B). We interpret this behavior as the energetically dependent response of at least two dityrosine chromophores with different lifetimes contributing to the overall fluorescence decay of intact yeast ascospores. The relatively broad distributions refer, moreover, to a multitude of dityrosine chromophores, contributing to each lifetime distribution, which differ marginally but significantly from the mean electronic transition rate. From independent experiments concerning the iodination of dityrosine in spore walls, principally two different dityrosine species—one solvent-accessible and one not accessible to solvent—were detected (Briza et al., 1990a).

From Fig. 4 B, one can see that there is also a small contribution of lifetimes at 4–5 ns resolvable in the decay. The distribution centered at  $\tau_2^c = 2.6$  ns in Fig. 3 B also shows a slight asymmetry with a tail to longer values. This may be due to the precursor successor/photophysics proposed for dityrosine in water (Kungl et al., 1992), according to which

these (unresolved) lifetimes refer to the emission of the two respective excited species of the chromophore.

However, the relative contributions of the two main lifetime distributions centered at  $\tau_1^c$  and  $\tau_2^c$  are emission wavelength dependent (Fig. 4). The two distributions, therefore, are the fluorescence responses of two energetically different dityrosine chromophore classes. To see whether these two species are also different in their location within the spore wall, we have tried to quench the spore fluorescence with acrylamide (Eftink, 1991b). Because this substance is soluble in water one might be able to differentiate between chromophores accessible to solvent and chromophores hidden from solvent. When acrylamide up to a concentration of 0.4 M is added to a spore suspension, a nonlinear Stern-Volmer plot is the result (Fig. 5). Several trials to adjust the data to modified equations (Eftink, 1991b) failed. No linear plot of the data could be obtained. Since we were not investigating two distinct dityrosine chromophores, but rather two broad ranges of topologically and energetically different dityrosine chromophores (Gryczynski et al., 1988), as is reflected in the distributional widths of decay time analysis (ESM) and rotational correlation time analysis (MEM), a linear dependence of  $F_0/F$  on the quencher concentration in any Stern-Volmer kinetics could not be expected.

When we applied ESM analysis to the quenched time-resolved fluorescence data sets, we found a shift of  $\tau_2^c$  to shorter values and a massive decrease of the long-lived component when the concentration of acrylamide is increased. Thus, this quencher meets with the solvent-accessible fraction of dityrosine chromophores in the spore wall during its fluorescence lifetime, thereby shortening this value and decreasing their contribution to the overall fluorescence decay. The estimated bimolecular rate constant  $k_q = 1.19 \times 10^9 \text{ M}^{-1} \text{ s}^{-1}$  is smaller than the one found for quenching dityrosine fluorescence in solution with acrylamide ( $k_q = 2.81 \times 10^9 \text{ M}^{-1} \text{ s}^{-1}$ ; A. J. Kungl, unpublished results). This difference refers to the influence of the yeast spore matrix on the free diffusion of the quencher to the chromophore. No influence on  $\tau_1^c$  could be detected. This is due to the dityrosine fraction, which is protected against the aqueous quencher.

We are not able to interpret the effect of KI on the spore fluorescence (data not shown) because the fluorescence linearly increases up to a concentration of 0.2 M KI. With higher concentrations of this compound, a slight decrease of the spore fluorescence has been observed. We hypothesize that intercalation of  $\text{I}^-$  ions into the polypeptide matrix enhances fluorescence by suppressing nonradiative deactivation pathways (matrix collisions, energy transfer, etc.).

The two dityrosine chromophore classes have also been characterized by their different mobilities in the spore wall (Lakowicz et al., 1983). This is revealed by time-resolved fluorescence anisotropy measurements (Bucci and Steiner, 1988). A long rotational correlation time of 30 ns has been found with a contribution to the overall decay of 75%. This long rotational correlation time reflects a slow segmental motion of the solvent accessible part of the spore wall. A broad range of mobility is manifested in the broad distribu-

tion of correlation times centered at 40 ns in the MEM analysis of the time-resolved anisotropy decay data (Fig. 6). The 0.9 ns rotational correlation time which has been found with a contribution of 25% can be attributed to the fast local motion of either dityrosine class. The corresponding very narrow rotational correlation time distribution at 0.7 ns (Fig. 6) refers to a uniform, but relatively long lasting, local dynamics of the chromophores in the macromolecular matrix (Munro et al., 1979).

Since we have shown here that the yeast spores contain two differently localized dityrosine species which differ in their spectral behavior, the question arises whether this serves a biological purpose. Ascospores of yeast are resistant to environmental influences like temperature, mutagenic UV light, and digestive enzymes. Most other fungal spores are protected from the mutagenic effects of UV light by pigments (melanin), which are contained in their outer walls. Yeast ascospores lack such pigments in their outer walls and, therefore, are nearly colorless. Dityrosine could functionally replace these pigments because of its absorption spectrum at 300–320 nm. This corresponds exactly to the part of the total spectrum at sea level that is responsible for the mutagenic action of sunlight (R. J. van Borstel, personal communication). Dityrosine excitation by UV light results in fluorescence at 404 nm, which is no more harmful to the DNA of the spore. The energetically higher fraction of UV light could be absorbed by the dityrosine species, which is contained in an aprotic environment and could then be transferred to the aqueous dityrosine species by energy transfer. Dityrosine has already been shown to be responsible for the resistance against the attack of degrading enzymes (Briza et al., 1990b). We propose here that, in addition, dityrosine may aid in the protection of the yeast spore genome from mutagenic UV light.

The authors wish to thank S. Marinits and A. van Hoek for technical assistance and G. Landl and H. W. Engl for the work on the development of the ESM algorithm.

This work was supported by the Österreichischen Fonds zur Förderung der wissenschaftlichen Forschung (project P7182).

## REFERENCES

- Alcala, J. R., E. Gratton, and F. G. Prendergast. 1987a. Resolvability of fluorescence lifetime distributions using phase fluorometry. *Biophys. J.* 51:587–596.
- Alcala, J. R., E. Gratton, and F. G. Prendergast. 1987b. Fluorescence lifetime distributions in proteins. *Biophys. J.* 51:597–604.
- Alcala, J. R., E. Gratton, and F. G. Prendergast. 1987c. Interpretation of fluorescence decays in proteins using continuous lifetime distributions. *Biophys. J.* 51:925–936.
- Beechem, J. M., and L. Brand. 1985. Time-resolved fluorescence of proteins. *Annu. Rev. Biochem.* 54:43–71.
- Briza, P., A. Ellinger, G. Winkler, and M. Breitenbach. 1986. Dityrosine is a prominent member of the yeast ascospore wall. *J. Biol. Chem.* 261:4288–4294.
- Briza, P., A. Ellinger, G. Winkler, and M. Breitenbach. 1990a. Characterization of a D,L-dityrosine-containing macromolecule from yeast spore walls. *J. Biol. Chem.* 265:15118–15123.
- Briza, P., M. Breitenbach, A. Ellinger, and J. Segall. 1990b. Regulation of two developmentally regulated genes involved in spore wall maturation in *Saccharomyces cerevisiae*. *Genes Dev.* 4:1775–1789.



- Bucci, E., and R. F. Steiner. 1988. Anisotropy decay of fluorescence as an experimental approach to protein dynamics. *Biophys. Chem.* 30:199–204.
- Creed, D. 1984a. The photophysics and photochemistry of the near UV absorbing amino acids. I. Tryptophan and its simple derivatives. *Photochem. Photobiol.* 39:537–562.
- Creed, D. 1984b. The photophysics and photochemistry of the near UV absorbing amino acids. II. Tyrosine and its simple derivatives. *Photochem. Photobiol.* 39:563–575.
- Demchenko, A. P. 1992. Fluorescence and dynamics in proteins. In *Topics in Fluorescence Spectroscopy*. Vol. 3. J. R. Lakowicz, editor. Plenum Press, New York. 65–111.
- Eftink, M. R. 1991a. Fluorescence techniques for studying protein structure. In *Methods of Biochemical Analysis*. Vol. 35. C. H. Suelter, editor. John Wiley Sons, New York. 127–204.
- Eftink, M. R. 1991b. Fluorescence quenching: theory and applications. In *Topics in Fluorescence Spectroscopy*. Vol. 2. J. R. Lakowicz, editor. Plenum Press, New York. 53–126.
- Esposito, R. E., M. Dresser, and M. Breitenbach. 1991. Identifying sporulation genes, visualizing synaptonemal complexes, and large-scale spore and spore wall purification. *Methods Enzymol.* 194:110–131.
- Foerder, C. A., and B. M. Shapiro. 1977. Release of ovoperoxidase from sea urchin eggs hardens the fertilization membrane with dityrosine cross-links. *Proc. Natl. Acad. Sci. USA.* 74:4214–4218.
- Gryczynski, I., M. Eftink, and J. R. Lakowicz. 1988. Conformation heterogeneity in proteins as an origin of heterogeneous fluorescence decays, illustrated by native and denatured ribonuclease T<sub>1</sub>. *Biochim. Biophys. Acta.* 954:244–252.
- Harris, D. L., and B. S. Hudson. 1990. Photophysics of tryptophan in bacteriophage T4 lysozyme. *Biochemistry.* 29:5276–5285.
- Hartig, A., R. Schroeder, E. Mucke, and M. Breitenbach. 1981. Isolation and characterization of yeast mitochondrial mutants defective in spore germination. *Curr. Genet.* 4:29–36.
- Hutnik, C. M., and A. G. Szabo. 1989. Confirmation that multiexponential fluorescence decay behavior of holoazurin originates from conformational heterogeneity. *Biochemistry.* 28:3923–3934.
- James, D. R., and W. R. Ware. 1985. A fallacy in the interpretation of fluorescence parameters. *Chem. Phys. Lett.* 120:455–459.
- James, D. R., and W. R. Ware. 1986. Recovery of underlying distributions of lifetimes from fluorescence decay data. *Chem. Phys. Lett.* 126:7–11.
- Kungl, A. J., G. Landl, A. J. W. G. Visser, M. Breitenbach, and H. F. Kauffmann. 1992. L-dityrosine: a time-resolved fluorescence investigation. *J. Fluorescence.* 2:63–74.
- Lakowicz, J. R., B. P. Maliwal, H. Cherek, and A. Balter. 1983. Rotational freedom of tryptophan residues in proteins and peptides. *Biochemistry.* 22:1741–1752.
- Landl, G., T. Langthaler, H. W. Engl, and H. F. Kauffmann. 1991. Distribution of event times in time-resolved fluorescence: the exponential series approach—algorithm, regularization, analysis. *J. Comp. Phys.* 95:1–28.
- Livesey, A. K., and J.-C. Brochon. 1987. Analyzing the distribution of decay constants in pulse-fluorometry using the maximum entropy method. *Biophys. J.* 52:693–706.
- Merola, F., R. Rigler, A. Holmgren, and J.-C. Brochon. 1989. Picosecond tryptophan fluorescence of thioredoxin: evidence for discrete species in slow exchange. *Biochemistry.* 28:3383–3398.
- Munro, I., I. Pecht, and L. Stryer. 1979. Subnanosecond motions of tryptophan residues in proteins. *Proc. Natl. Acad. Sci. USA.* 76:55–60.
- O'Connor, D. V., and D. Phillips. 1984. *Time-Correlated Single Photon Counting*. Academic Press, London. 288 pp.
- Royer, C. A., J. A. Gardner, J. M. Beechem, J.-C. Brochon, and K. S. Matthews. 1990. Resolution of the fluorescence decay of the two tryptophan residues of lac repressor using single tryptophan mutants. *Biophys. J.* 58:363–378.
- Royer, C. A. 1993. Understanding fluorescence decay in proteins. *Biophys. J.* 65:9–10.
- Skilling, J., and S. F. Gull. 1985. Algorithms and applications. In *Maximum-Entropy and Bayesian Methods in Inverse Problems*. C. R. Smith and W. T. Grandy, editors. D. Reidel, Dordrecht. 83–133.
- van Hoek, A., and A. J. W. G. Visser. 1981. Pulse selection system with electro-optic modulators applied to mode-locked CW lasers and time-resolved single photon counting. *Rev. Sci. Instr.* 52:1199–1205.
- van Hoek, A., K. Vos, and A. J. W. G. Visser. 1987. Ultrasensitive time-resolved polarized fluorescence spectroscopy as a tool in biology and medicine. *IEEE J. Quant. Electr.* 10:1812–1820.
- Vincent, M., J.-C. Brochon, F. Merola, W. Jordi, and J. Gallay. 1988. Nanosecond dynamics of horse heart apocytochrome c in aqueous solution as studied by time-resolved fluorescence of the single tryptophan residue (Trp-59). *Biochemistry.* 27:8752–8761.
- Visser, A. J. W. G., T. Kulinski, and A. van Hoek. 1988. Fluorescence lifetime measurements of pseudoazulenes using picosecond-resolved single photon counting. *J. Mol. Struct.* 175:111–116.
- Vos, K., A. van Hoek, and A. J. W. G. Visser. 1987. Applications of a reference convolution method to tryptophan fluorescence in proteins. A refined description of rotational dynamics. *Eur. J. Biochem.* 165:55–63.